Unexpected Gold-containing Boride Clusters formed from the Reactions of $[RhRu_3H(\eta^5\text{-}C_5Me_5)(CO)_9BH]^-$ with Gold(I) Phosphine Derivatives: Crystal Structures of $[RhRu_3H(\eta^5\text{-}C_5Me_5)(CO)_9B\{Au(PPh_3)\}_2(AuCl)]\cdot CH_2Cl_2$ and $[RhRu_3H(\eta^5\text{-}C_5Me_5)(CO)_9B\{Au_2(dppf)\}(AuCl)]\cdot CH_2Cl_2$ [dppf = 1,1′-bis(diphenylphosphino)ferrocene]†

Jane R. Galsworthy,[a] **Catherine E. Housecroft***[,b] **and Arnold L. Rheingold***[,c]

[a] *University Chemical Laboratory, Lensfield Road, Cambridge CB2 1EW, UK*
[b] *Institut für Anorganische Chemie, Spitalstrasse 51, CH-4056 Basel, Switzerland*
[c] *Department of Chemistry, University of Delaware, Newark, DE 19716, USA*

The deprotonation of $[RhRu_3H(\eta^5\text{-}C_5Me_5)(CO)_9BH_2]$ occurred by loss of an M–H–B bridging hydrogen atom to give $[RhRu_3H(\eta^5\text{-}C_5Me_5)(CO)_9BH]^-$ **1**; indirect evidence suggests the Rh–H–B proton has been removed. Anion **1** reacts with $[AuCl(PPh_3)]$ or $[Au_2Cl_2(dppf)]$ [dppf = 1,1′-bis(diphenylphosphino)ferrocene] to yield $[RhRu_3H(\eta^5\text{-}C_5Me_5)(CO)_9B\{Au(PPh_3)\}_2(AuCl)]$ **2** and $[RhRu_3H(\eta^5\text{-}C_5Me_5)(CO)_9B\{Au_2(dppf)\}(AuCl)]$ **3** respectively rather than expected derivatives of the type $[RhRu_3(\eta^5\text{-}C_5Me_5)(CO)_9BH_{3-x}(AuL)_x]$ (x = 1, 2 or 3). The single crystal structures of **2**$\cdot CH_2Cl_2$ and **3**$\cdot CH_2Cl_2$ have been determined: **2**$\cdot CH_2Cl_2$, monoclinic, space group $P2_1/c$, a = 11.944(4), b = 40.870(6), c = 13.313(4) Å, β = 108.66(2)°, Z = 4, R = 0.0684; **3**$\cdot CH_2Cl_2$, monoclinic, space group $P2_1/c$, a = 11.919(2), b = 39.350(8), c = 13.520(4) Å, β = 108.62(2)°, Z = 4, R = 0.0584. The trigold derivative $[RhRu_3(\eta^5\text{-}C_5Me_5)(CO)_9B\{Au(PPh_3)\}_3]$ was formed either by treating **1** with $[\{Au(PPh_3)\}_3O][BF_4]$ or treating **2** with PPh_3 in the presence of $Tl[PF_6]$ or $[N(PPh_3)_2]Cl$. The chloride ligand in compound **2** was replaced by iodide through reaction with $[NEt_4]I$. Anion **1** also reacted with $[Au_2Cl_2(dppa)]$ [dppa = bis(diphenylphosphino)acetylene] to give the linked dicluster species $[\{RhRu_3H(\eta^5\text{-}C_5Me_5)(CO)_9B(AuCl)\}_2\{\mu\text{-}Au(dppa)Au\}_2]$.

The replacement of a proton by a $\{Au(PR_3)\}^+$ unit is a well established synthetic procedure.[1] In a large number of monogold derivatives of transition-metal clusters, where structural comparisons are possible, the $\{Au(PR_3)\}^+$ unit (R = alkyl or aryl) and the proton it replaces adopt similar positions on the cluster surface. This analogy often breaks down for di- and tri-gold-substituted clusters and there is a noticeable tendency for the gold atoms to occupy adjacent sites in the metal cage, this being concomitant with the formation of gold–gold bonding interactions.

In transition metal clusters that incorporate a p-block element in an exposed (*e.g.* semi-interstitial) site, the $\{Au(PR_3)\}^+$ units have the option of interacting with either the metal and/or main-group atom sites. A recent example shows the propensity of $\{Au(PPh_3)\}^+$ electrophiles (a maximum of four) to bind to the phosphorus atom of the $[Fe_3(CO)_9P]^{3-}$ core.[2] We have illustrated that the semi-interstitial boron atom in M_4B-butterfly clusters (M = Fe or Ru) is also a centre around which $\{Au(PR_3)\}^+$ units aggregate.[3–6] One example which breaks this trend is $[Ru_4(CO)_{12}BH\{AuP(C_6H_4Me\text{-}2)_3\}_2]$.[5] Spectroscopic data are consistent with one of two isomers of this compound possessing a structure in which the two gold atoms are remote from one another and in which only one of the gold atoms bonds to the boron atom. This structure is not dissimilar from those of $[Ru_4(CO)_{12}C\{Au(PMe_2Ph)\}_2]$ and $[Ru_4(CO)_{12}C\{Au(PPh_3)\}_2]$.[7]

Particularly relevant to the present discussion are two results from our work. The first is the formation of the trigold derivative $[Fe_4(CO)_{12}B\{Au(PPh_3)\}_3]$ through the reaction of $[Fe_4H(CO)_{12}BH]^-$ with $[AuCl(PPh_3)]$ or $[\{Au(PPh_3)\}_3O]^+$. The crystal structure of $[Fe_4(CO)_{12}B\{Au(PPh_3)\}_3]$ confirms the aggregation of the three gold(I) moieties around the boron atom [Fig. 1(*a*)].[8] The second result is the reaction of $[M_4H(CO)_{12}BH]^-$ (M = Fe or Ru) with $[Au_2Cl_2(dppf)]$ which leads to $[M_4H(CO)_{12}B\{Au_2(dppf)\}]$. The exact cluster structure depends upon M; for M = Ru the cluster core is shown in Fig. 1(*b*). For M = Fe, an equilibrium exists in

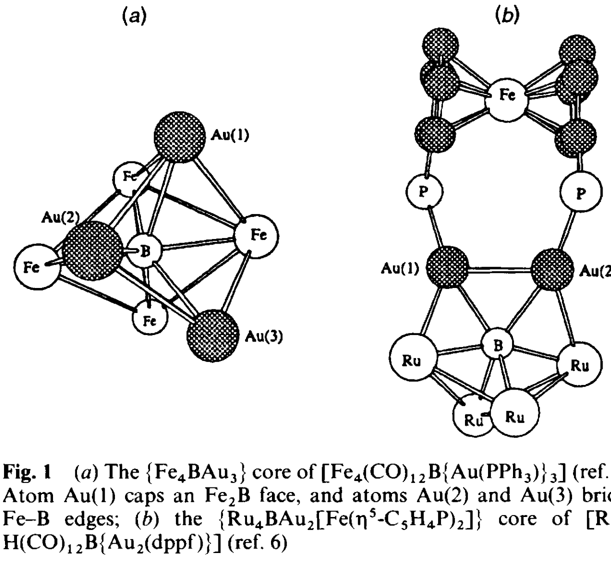

Fig. 1 (*a*) The $\{Fe_4BAu_3\}$ core of $[Fe_4(CO)_{12}B\{Au(PPh_3)\}_3]$ (ref. 8). Atom Au(1) caps an Fe_2B face, and atoms Au(2) and Au(3) bridge Fe–B edges; (*b*) the $\{Ru_4BAu_2[Fe(\eta^5\text{-}C_5H_4P)_2]\}$ core of $[Ru_4H(CO)_{12}B\{Au_2(dppf)\}]$ (ref. 6)

---

† *Supplementary data available:* see Instructions for Authors, *J. Chem. Soc., Dalton Trans.*, 1995, Issue 1, pp. xxv–xxx.

solution between an isomer with an analogous structure and a second isomer in which the {Au_2(dppf)} unit is less symmetrically bound to the cluster. In both isomers, both Au atoms are bonded to the boron atom. Further, the formation of [$Ru_4H(CO)_{12}B$\{Au_2(dppf)\}] competes with a pathway that gives the linked species [\{$Ru_4H(CO)_{12}B$\}$_2$\{μ-Au(dppf)Au\}].[6]

In this paper we detail the results of the reactions of a heterometallic boron-containing butterfly cluster with several gold(I) complexes containing mono- or di-dentate phosphine ligands. Our interest was to investigate the degree to which the presence of the heterometal atom perturbs the electronic structure and reactivity patterns of the cluster with respect to the all-ruthenium analogue. The precursor for these reactions is [$RhRu_3H(\eta^5$-$C_5Me_5)(CO)_9BH]^-$. We have previously reported the synthesis of [$RhRu_3H(\eta^5$-$C_5Me_5)(CO)_9BH_2$]; the rhodium atom resides in a wing-tip site in the butterfly core.[9]

Experimental

General.—Fourier transform NMR spectra were recorded on a Bruker WM 250 or AM 400 spectrometer. Proton NMR shifts are reported with respect to δ 0 for $SiMe_4$; ^{11}B with respect to δ 0 for $BF_3{\cdot}OEt_2$; ^{31}P with respect to δ 0 for H_3PO_4. All downfield chemical shifts are positive. Infrared spectra were recorded on a Perkin-Elmer FT 1710 spectrophotometer and FAB (fast atom bombardment) and FIB (fast ion bombardment) spectra on Kratos instruments with 3-nitrobenzyl alcohol as matrix.

All reactions were carried out under argon by using standard Schlenk techniques. Solvents were dried over suitable reagents and freshly distilled under N_2 before use. Separations were carried out by thin-layer plate chromatography with Kieselgel 60-PF-254 (Merck). The reagents [$N(PPh_3)_2$]Cl, [NEt_4]I and PPh_3 were used as received (Aldrich). The compounds [$RhRu_3H(\eta^5$-$C_5Me_5)(CO)_9BH_2$],[9] [$AuCl(PPh_3)$],[10,11] [Au_2Cl_2(dppf)],[12] [Au_2Cl_2(dppa)][13] and [\{$Au(PPh_3)$\}$_3$O][BF_4][14] were prepared according to published methods. Yields are with respect to the starting cluster anion **1** for the preparations of **2**, **3**, **4**, **6** (method C) and **7**, or with respect to the appropriate derivative cluster for the preparations of **5** and **6** (methods A and B). The yields given are typical values and vary slightly from one reaction to another.

Preparations.—[$N(PPh_3)_2$][$RhRu_3H(\eta^5$-$C_5Me_5)(CO)_9BH$]. A methanolic solution (10 cm^3) of [$N(PPh_3)_2$]Cl (57 mg, 0.1 mmol) and Na_2CO_3 (8 mg, 0.08 mmol) was added to a solution of [$RhRu_3H(\eta^5$-$C_5Me_5)(CO)_9BH_2$][9] (81 mg, 0.1 mmol) in CH_2Cl_2 (5 cm^3). The solution was stirred for 15 min during which time it turned dark brown. The solvent was removed *in vacuo* and the product was extracted into diethyl ether. Deprotonation of [$RhRu_3H(\eta^5$-$C_5Me_5)(CO)_9BH_2$] was close to quantitative. NMR ($CDCl_3$, 298 K): ^1H (400 MHz) δ +7.7–7.3 (m, Ph), +1.88 (s, Me), −4.9 (br, M–H–B, M = Ru or Rh; see text), −20.17 (s, Ru–H–Ru); ^{11}B (128 MHz), δ +149. IR (CH_2Cl_2, cm^{-1}): ν_{CO} 2034m, 1999s, 1971vs, 1959s (sh), 1757w.

[$RhRu_3H(\eta^5$-$C_5Me_5)(CO)_9B$\{$Au(PPh_3)$\}$_2$(AuCl)] **2**. The [$N(PPh_3)_2]^+$ salt of **1** (134 mg, 0.1 mmol) was dissolved in CH_2Cl_2 (5 cm^3) and one equivalent of [$AuCl(PPh_3)$] (50 mg, 0.1 mmol) was added. The brown solution was stirred for 30 min. The solvent volume was reduced to 2 cm^3 and the reaction mixture separated by TLC, eluting with hexane–CH_2Cl_2 (1 : 2). Cluster **2** (red-brown) was initially isolated in ≈30% yield as the second fraction; after their isolation, the first and third fractions rapidly converted to **2** whilst standing in solution, or on storage as a solid at ≈5 °C. NMR ($CDCl_3$, 298 K): ^1H (400 MHz), δ +7.7–7.2 (m, Ph), +2.07 (s, Me), −18.86 (s, Ru–H–Ru); ^{11}B (128 MHz), δ +158; ^{31}P (162 MHz), δ +57.5 (s, 1 P), +43.4 (s, 1 P). IR (CH_2Cl_2, cm^{-1}): ν_{CO} 2058vs, 2026m, 2000vs, 1969w (sh), 1944w, 1788w. FAB mass spectrum: *m/z* 1958 (M^+) (Calc. for $^{12}C_{55}{}^1H_{46}{}^{197}Au_3{}^{11}B_1{}^{35}Cl_1{}^{16}O_9{}^{31}P_2{}^{103}Rh_1{}^{101}Ru_3$ 1955) with 9 CO losses.

[$RhRu_3H(\eta^5$-$C_5Me_5)(CO)_9B$\{Au_2(dppf)\}(AuCl)] **3**. The same method was used as for the preparation of compound **2**; [Au_2Cl_2(dppf)] (102 mg, 0.1 mmol) replaced [$AuCl(PPh_3)$]. Compound **3** (red-brown) was separated in ≈70% yield as the second fraction. NMR ($CDCl_3$, 298 K): ^1H (400 MHz), δ +7.7–7.2 (m, Ph), +5.3, +4.3, +3.9, +3.5 (all br, C_5H_5), +2.07 (s, Me), −18.65 (s, Ru–H–Ru); ^{11}B (128 MHz), δ +158; ^{31}P (162 MHz), δ +50.8 (s, 1 P), +36.2 (s, 1 P). IR (CH_2Cl_2, cm^{-1}) ν_{CO} 2058vs, 2025m, 1999vs, 1966w (sh), 1942w, 1785w. FAB mass spectrum: *m/z* 1989 (M^+) (Calc. for $^{12}C_{53}{}^1H_{44}{}^{197}Au_3{}^{11}B_1{}^{35}Cl_1{}^{56}Fe_1{}^{16}O_9{}^{31}P_2{}^{103}Rh_1{}^{101}Ru_3$ 1985) with 8 CO losses.

[\{$RhRu_3H(\eta^5$-$C_5Me_5)(CO)_9B$(AuCl)\}$_2$\{μ-Au(dppa)Au\}$_2$] **4**. The procedure was as for **2** with [Au_2Cl_2(dppa)] (90 mg, 0.1 mmol) replacing [$AuCl(PPh_3)$]. Compound **4** (brown) was isolated in ≈50% yield and was the only fraction eluted. NMR ($CDCl_3$, 298 K): ^1H (400 MHz), δ +7.8–7.3 (m, Ph), +2.05 (s, Me), −19.19 (s, Ru–H–Ru); ^{11}B (128 MHz), δ +159; ^{31}P (162 MHz), δ +33.2 (s, 1 P), +23.7 (s, 1 P). IR (CH_2Cl_2, cm^{-1}) ν_{CO} 2059s, 2029s, 2000vs, 1947w, 1791w. FAB mass spectrum: *m/z* 3654 (M^+) (Calc. for $^{12}C_{90}{}^1H_{72}{}^{197}Au_6{}^{11}B_2{}^{35}Cl_2{}^{16}O_{18}{}^{31}P_4{}^{103}Rh_2{}^{101}Ru_6$ 3650).

[$RhRu_3H(\eta^5$-$C_5Me_5)(CO)_9B$\{$Au(PPh_3)$\}$_2$(AuI)] **5**. A solution of [NEt_4]I (26 mg, 0.1 mmol) in CH_2Cl_2 (5 cm^3) was added to a solution of compound **2** (98 mg, 0.05 mmol) in CH_2Cl_2 (5 cm^3), and was stirred for 1 h. The solvent volume was reduced to 2 cm^3 *in vacuo* and products were separated by TLC eluting with CH_2Cl_2–hexane (2 : 1). One fraction (brown) was isolated in ≈80% yield and identified as **5**. A second fraction (brown) remains uncharacterised. NMR ($CDCl_3$, 298 K): ^1H (400 MHz), δ +7.7–7.3 (m, Ph), +2.05 (s, Me), −18.77 (s, Ru–H–Ru); ^{11}B (128 MHz), δ +158. IR (CH_2Cl_2, cm^{-1}) ν_{CO} 2058vs, 2026m, 2000vs, 1969w (sh), 1944w, 1788w. FIB mass spectrum: *m/z* 2048 (M^+) (Calc. for $^{12}C_{55}{}^1H_{46}{}^{197}Au_3{}^{11}B_1{}^{127}I_1{}^{16}O_9{}^{31}P_2{}^{103}Rh_1{}^{101}Ru_3$ 2047) with 8 CO losses.

[$RhRu_3(\eta^5$-$C_5Me_5)(CO)_9B$\{$Au(PPh_3)$\}$_3$] **6**. *Method A*. Compound **2** (100 mg, 0.05 mmol) was dissolved in CH_2Cl_2 (5 cm^3) and solid [$N(PPh_3)_2$]Cl (58 mg, 0.1 mmol) added; IR spectroscopic data indicated that no change had occurred after 15 min stirring. Triphenylphosphine (260 mg, 0.1 mmol) was added to the reaction mixture and the solution was stirred for 20 min. Solvent was removed *in vacuo* and the products were separated by TLC using CH_2Cl_2–hexane (2 : 1). Compound **6** (brown) was isolated in ≈70% yield with the remainder of the product being present as a brown, intractable baseline.

Method B. Compound **2** (98 g, 0.05 mmol) was dissolved in CH_2Cl_2 (5 cm^3) and solid Tl[PF_6] (34 mg, 0.1 mmol) was added. After 45 min stirring, the IR spectrum indicated that no reaction had occurred. Triphenylphosphine (520 mg, 0.2 mmol) was added and the solution stirred for 30 min. The solvent was removed *in vacuo* and the mixture separated by TLC using CH_2Cl_2–hexane (2 : 1). Compound **6** (brown) was isolated in ≈70% yield with the remainder of the product being present as a brown, intractable baseline.

Method C. A solution of [\{$Au(PPh_3)$\}$_3$O][BF_4] (40 mg, 0.03 mmol) dissolved in CH_2Cl_2 (5 cm^3) was added to a solution of [$N(PPh_3)_2$][$RhRu_3H(\eta^5$-$C_5Me_5)(CO)_{12}BH$] (130 mg, 0.1 mmol) in CH_2Cl_2 (5 cm^3). After 15 min stirring, the solvent was removed *in vacuo*. The products were separated by TLC using CH_2Cl_2–hexane (1 : 1). The first (brown) fraction was identified as [$RhRu_3H_2(\eta^5$-$C_5Me_5)(CO)_9B$\{$Au(PPh_3)$\}] **7** (≈30%). The second fraction was characterised as compound **6** (≈40%), and the final fraction was **2** (≈25%).

[$RhRu_3(\eta^5$-$C_5Me_5)(CO)_9B$\{$Au(PPh_3)$\}$_3$] **6**. NMR ($CDCl_3$, 298 K): ^1H (400 MHz), δ +7.7–7.3 (m, Ph), +2.05 (s, Me); ^{11}B (128 MHz), δ +167; ^{31}P (162 MHz), δ +53.5 (s). IR (CH_2Cl_2, cm^{-1}) ν_{CO} 2042m, 2006s, 1981vs, 1942w, 1774w. FAB mass spectrum: *m/z* 2183 (M^+) (Calc. for $^{12}C_{73}{}^1H_{60}{}^{197}Au_3{}^{11}B_1{}^{16}O_9{}^{31}P_3{}^{103}Rh_1{}^{101}Ru_3$ 2181) with loss of \{$Au(PPh_3)$\}$^+$ and 8 CO losses.

[$RhRu_3H_2(\eta^5$-$C_5Me_5)(CO)_9B$\{$Au(PPh_3)$\}] **7**. NMR

($CDCl_3$, 298 K): ^1H (400 MHz), δ +7.7–7.2 (m, Ph), +1.95 (s, Me), −14.5 (br, M–H–M′, M′ = Ru or Rh, see text), −20.4 (br, M–H–M′, M′ = Ru or Rh, see text); ^{11}B (128 MHz), δ +174; ^{31}P (162 MHz), δ +56.3 (s). IR (CH_2Cl_2, cm^{-1}) ν_{CO} 2065s, 2024vs, 2005m (sh), 1965w, 1794w. FAB mass spectrum: *m/z* 1266 (M^+) (Calc. for $^{12}C_{37}{}^{1}H_{32}{}^{197}Au_1{}^{11}B_1{}^{16}O_9{}^{31}P_1{}^{103}Rh_1{}^{101}Ru_3$ 1265) with 9 CO losses.

Crystal Structural Determinations.—Crystallographic data for **2**·CH_2Cl_2 and **3**·CH_2Cl_2 are collected in Table 1. Crystals of both were mounted on glass fibres and from photographic characterisation were found to be monoclinic. For both, systematic absences in the data uniquely indicated the space group $P2_1/c$. Corrections for absorption were made using empirical ψ-scan data. Direct methods were used to solve the structures. In both cases a molecule of dichloromethane, one of the crystallisation solvents, was found accompanying the cluster. For **2**, the solvent molecule was disordered; however, for **3**, the solvent molecule was severely disordered and proved to be impossible to model successfully. Therefore, a definitive confirmation of chemical identity was not possible, but circumstantial evidence strongly supports dichloromethane. This is based upon the location and shape of the solvent cavity. Of the two solvents used for crystallisation, CH_2Cl_2 and hexane, only the former could be accommodated. Crude modelling was achieved by allowing six clustered carbon atoms, C(101)–C(106) to represent fractionally occupied C and Cl positions. Additionally, four of the top six unassigned electron density peaks (0.8–1.2 e $Å^{-3}$) also reside in the solvent cluster.

In **2**, only metallic atoms and the Cl atom bonded to Au were anisotropically refined; in **3**, all non-hydrogen atoms except for those associated with the disordered solvent molecule were anisotropically refined. No constraints were applied to the phenyl rings. Hydrogen atoms were treated as idealised contributions, except for solvent in **3** for which these contributions were ignored.

All computations used the SHELXTL-PC software.[15] Atomic coordinates for **2** and **3** are given in Tables 2 and 3, respectively.

Additional material available from the Cambridge Crystallographic Data Centre comprised H-atom coordinates, thermal parameters and remaining bond lengths and angles.

Results and Discussion

Deprotonation of $[RhRu_3H(\eta^5\text{-}C_5Me_5)(CO)_9BH_2]$.—The neutral heterometallaborane $[RhRu_3H(\eta^5\text{-}C_5Me_5)(CO)_9BH_2]$[9] is readily deprotonated upon treatment with sodium carbonate, and the monoanion $[RhRu_3H(\eta^5\text{-}C_5Me_5)(CO)_9BH]^-$ **1** has been isolated as the $[N(PPh_3)_2]^+$ salt. The ^{11}B NMR spectrum of $[RhRu_3H(\eta^5\text{-}C_5Me_5)(CO)_9BH_2]$ exhibits a signal at δ +94.0 and the mid- to high-field region of the ^1H NMR spectrum is characterised by resonances at δ −20.29 (assigned to the hinge bridging Ru–H–Ru proton) and δ −9.6 (two overlapping signals assigned to the Ru–H–B and Rh–H–B bridges).[9] The ^{11}B NMR spectral resonance for monoanion **1** is at δ +149 and the downfield shift upon deprotonation is consistent with the loss of a boron-bound proton.[16] No ^{11}B–^1H coupling could be resolved to confirm this. In the ^1H NMR spectrum of **1**, a sharp singlet at δ −20.17 indicates that the Ru–Ru hinge-bridging hydrogen atom has been retained. In the M–H–B region of the spectrum, a broad signal at δ −4.9 indicates the presence of *either* an Ru–H–B *or* Rh–H–B bridge, but in the absence of resolved ^1H–^{103}Rh coupling we are unable to distinguish between the two possibilities. The structure shown has a Ru–H–B bridge, and indirect evidence for this choice is presented below.

Reactions of $[RhRu_3H(\eta^5\text{-}C_5Me_5)(CO)_9BH]^-$ **1** *with* $[AuCl(PPh_3)]$ *and* $[Au_2Cl_2(dppf)]$.—The $[N(PPh_3)_2]^+$ salt of **1** reacts smoothly with $[AuCl(PPh_3)]$ to give a neutral product **2** as the major species. Several minor fractions which were collected during chromatographic separation rapidly converted to **2**. Similarly (see Scheme 1), **1** reacts with $[Au_2Cl_2(dppf)]$ to give neutral **3**. Each of the compounds **2** and **3** is characterised in solution by a broad ^{11}B NMR spectral resonance at δ +158. This shift is relatively close to that of the starting material (δ +149) and this suggests that the boron atom remains within

Table 1 Crystallographic data for **2**·CH_2Cl_2 and **3**·CH_2Cl_2[a]

	2·CH_2Cl_2	**3**·CH_2Cl_2
Formula	$C_{55}H_{46}Au_3BClO_9P_2RhRu_3\cdot CH_2Cl_2$	$C_{53}H_{44}Au_3BClFeO_9P_2RhRu_3\cdot CH_2Cl_2$
Formula weight	2040.1	206 9.9
a/Å	11.944(4)	11.919(2)
b/Å	40.870(6)	39.350(8)
c/Å	13.313(4)	13.520(4)
β/°	108.66(2)	108.62(2)
U/Å^3	6157(2)	6009(2)
F(000)	3820	3700
Crystal dimensions/mm	0.10 × 0.12 × 0.24	0.18 × 0.32 × 0.32
Colour	dark red	dark red
D_c/g cm^{-3}	2.201	2.288
μ(Mo-Kα)/cm^{-1}	83.3	87.7
T/K	233	228
T_{max}, T_{min}	1.00, 0.46	1.00, 0.41
2θ Scan range/°	4–48	4–55
Reflections collected	9647	14592
Independent reflections	9239	13802
Independent observed reflections [$F_o \geqslant 5\sigma(F_o)$]	6112	8504
R[b]	0.0684	0.0584
R'[b]	0.0907	0.0721
Weighting scheme, w^{-1}	$\sigma^2(F) + 0.0013F^2$	$\sigma(F) + 0.0010F^2$
Δσ(maximum)	0.210	0.03
Δρ/e Å^{-3}	1.91	1.74
N_o/N_v[c]	16.8	12.3
Goodness of fit	1.63	1.40

[a] Details in common: monoclinic, space group $P2_1/c$, Z = 4; Siemens P4 diffractometer, graphite-monochromated Mo-Kα radiations (λ = 0.710 73 Å), three standard reflections every 197, with < 1% variation. [b] $R = \Sigma\Delta/\Sigma(F_o)$, $R' = \Sigma\Delta w^{\frac{1}{2}}/\Sigma(F_o w^{\frac{1}{2}})$, $\Delta = |(F_o - F_c)|$; quantity minimised = $\Sigma w\Delta^2$. [c] N_o = Number of observations, N_v = number of variables.

Table 2 Atomic coordinates (× 10^4) for **2**

Atom	*x*	*y*	*z*	Atom	*x*	*y*	*z*
Au(1)	4 369.1(9)	3 577.2(2)	2 588.7(8)	C(111)	3 516(26)	4 311(7)	862(23)
Au(2)	6 582.7(9)	3 830.3(2)	4 047.1(8)	C(112)	3 562(26)	4 621(7)	413(23)
Au(3)	6 523(1)	3 955.1(3)	6 121.4(8)	C(113)	3 474(32)	4 661(9)	−582(29)
Rh	7 786(2)	3 155.2(5)	5 819(2)	C(114)	3 239(36)	4 342(10)	−1 242(33)
Ru(1)	5 998(2)	3 152.7(5)	3 945(2)	C(115)	3 110(33)	4 038(9)	−788(28)
Ru(2)	4 610(2)	3 668.0(5)	4 775(2)	C(116)	3 252(24)	4 042(6)	250(21)
Ru(3)	5 471(2)	3 075.1(5)	5 912(2)	C(121)	849(33)	3 891(9)	598(27)
P(1)	3 119(6)	3 658(2)	894(5)	C(122)	−304(37)	3 867(10)	703(30)
P(2)	7 350(6)	4 249(2)	3 331(5)	C(123)	−693(30)	3 631(8)	949(24)
Cl	7 346(8)	4 363(2)	7 346(6)	C(124)	−37(42)	3 350(12)	1 197(35)
B	6 420(24)	3 476(6)	5 380(20)	C(125)	1 145(29)	3 379(8)	1 165(23)
O(1)	4 317(20)	2 718(5)	2 243(17)	C(126)	1 603(23)	3 649(6)	855(20)
O(2)	7 545(19)	3 267(5)	2 573(16)	C(131)	2 306(28)	3 249(7)	−882(23)
O(3)	7 483(17)	2 546(5)	4 570(14)	C(132)	2 428(33)	3 027(8)	−1 581(28)
O(4)	2 404(21)	3 264(5)	3 701(17)	C(133)	3 515(32)	2 867(9)	−1 445(29)
O(5)	3 844(16)	4 322(4)	3 673(14)	C(134)	4 465(26)	2 957(7)	−607(21)
O(6)	3 727(20)	3 819(5)	6 614(17)	C(135)	4 313(26)	3 209(7)	132(22)
O(7)	2 980(20)	2 822(5)	5 750(17)	C(136)	3 254(24)	3 355(7)	−18(20)
O(8)	6 044(20)	3 382(5)	8 122(18)	C(211)	6 881(26)	4 711(7)	4 633(22)
O(9)	6 620(18)	2 403(5)	6 623(15)	C(212)	6 368(23)	5 013(6)	4 841(20)
C(1)	4 970(23)	2 907(6)	2 866(20)	C(213)	5 693(28)	5 208(8)	4 016(23)
C(2)	6 948(23)	3 243(6)	3 107(20)	C(214)	5 518(25)	5 127(7)	2 975(21)
C(3)	7 196(21)	2 815(6)	4 693(18)	C(215)	6 037(23)	4 823(6)	2 784(21)
C(4)	3 255(26)	3 443(7)	4 098(21)	C(216)	6 742(22)	4 638(6)	3 596(19)
C(5)	4 202(22)	4 089(6)	4 119(19)	C(221)	9 631(26)	4 083(7)	3 455(22)
C(6)	4 080(26)	3 783(7)	5 911(22)	C(222)	10 856(28)	4 093(8)	3 864(23)
C(7)	3 934(28)	2 939(7)	5 828(23)	C(223)	11 391(35)	4 312(9)	4 598(28)
C(8)	5 852(26)	3 276(7)	7 306(23)	C(224)	10 793(28)	4 504(8)	5 038(24)
C(9)	6 242(29)	2 687(8)	6 390(24)	C(225)	9 521(24)	4 506(7)	4 620(21)
C(10)	9 101(29)	3 327(8)	7 370(25)	C(226)	8 940(24)	4 298(6)	3 804(20)
C(11)	9 219(33)	2 960(9)	7 234(29)	C(231)	7 541(23)	4 478(6)	1 376(19)
C(12)	9 575(28)	2 898(7)	6 430(24)	C(232)	7 299(27)	4 459(7)	317(22)
C(13)	9 685(25)	3 214(7)	5 910(22)	C(233)	6 591(26)	4 201(7)	−254(24)
C(14)	9 397(31)	3 435(8)	6 508(27)	C(234)	6 173(29)	3 944(8)	221(24)
C(15)	8 912(36)	3 488(9)	8 288(29)	C(235)	6 384(24)	3 979(6)	1 305(20)
C(16)	9 068(48)	2 726(13)	7 959(38)	C(236)	7 097(21)	4 240(6)	1 923(18)
C(17)	9 921(35)	2 590(9)	6 157(28)	C(0)	850(77)	4 974(21)	2 430(62)
C(18)	10 098(44)	3 205(12)	4 994(36)	Cl(A)	−369(22)	5 209(6)	2 252(18)
C(19)	9 646(34)	3 813(8)	6 400(29)	Cl(B)	934(24)	4 777(7)	1 504(21)

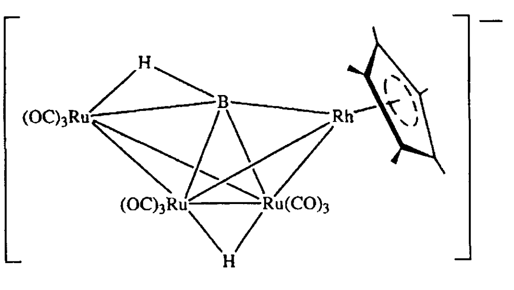

1

bonding contact of at least four metal atoms. The ^{31}P NMR spectrum of each new product displays two singlets of equal intensity (δ +57.5 and +43.4 for **2** and δ +50.8 and +36.2 for **3**). For **2**, this is consistent with the presence of two inequivalent {Au(PPh$_3$)} units and for **3**, the presence of an asymmetrically bound {Au(dppf)Au} unit. In the ^1H NMR spectrum of each compound, a singlet assignable to a ruthenium–ruthenium bridging hydrogen atom (for **2** δ −18.86 and for **3** −18.65) is observed.

These solution spectroscopic data initially indicated the formation of digold(I) derivatives of a type related to those of the tetraruthenium boron-containing butterfly cluster, *viz.* $[Ru_4H(CO)_{12}B\{Au(PPh_3)\}_2]$,[17] and $[Ru_4H(CO)_{12}B\{Au_2(dppf)\}]$.[6] However, mass spectral data for **2** and **3** were in accord with the additional presence of a {AuCl} unit in each case, giving formulae for the two compounds of $[RhRu_3H(\eta^5\text{-}C_5Me_5)(CO)_9B\{Au(PPh_3)\}_2(AuCl)]$ and $[RhRu_3H(\eta^5\text{-}C_5Me_5)(CO)_9B\{Au_2(dppf)\}(AuCl)]$ respectively. This unexpected result was confirmed by the results of single crystal X-ray analyses of **2** and **3**.

Crystal Structure of $[RhRu_3H(\eta^5\text{-}C_5Me_5)(CO)_9B\{Au(PPh_3)_2\}(AuCl)]\cdot CH_2Cl_2$ **2**·CH_2Cl_2.—Crystals of **2**·CH_2Cl_2, suitable for X-ray analysis, were grown at −25 °C from a CH_2Cl_2 solution layered with hexane. The molecular structure of **2** is shown in Fig. 2, and the structure of the cluster core is depicted in Fig. 3. Selected bond distances and angles are listed in Table 4. Cluster **2** retains a $RhRu_3$-butterfly core and the boron atom is within bonding contact of the four Group 8 and Group 9 metal atoms; Rh–B 2.03(3), and the Ru–B distances lie in the range 2.20–2.25(3) Å. The boron atom lies 0.35(2) Å above the $Rh_{wing\text{-}tip}$–$Ru(2)_{wing\text{-}tip}$ axis.

Compound **2** contains two {Au(PPh$_3$)} units. Atom Au(1) bridges the Ru(1)–Ru(2) edge, and atom Au(2) caps the Ru(1)Ru(2)B face. The distance between these two gold atoms is 2.923(2) Å, which is consistent with some degree of Au(1)–Au(2) bonding character. This arrangement of {Au(PPh$_3$)} units contrasts with that seen in $[Ru_4H(CO)_{12}B\{Au(PPh_3)\}_2]$,[17] in which both {Au(PPh$_3$)} fragments bind to the boron atom through Au–B interactions. Indeed, within a range of Fe_4BAu_x (x = 1–3) and Ru_4BAu_x (x = 1 or 2) butterfly compounds, we have observed that there is a general tendency for the gold atoms to be associated with the boron atom rather than solely with the metal framework.[3–6,17] An exception was

Table 3 Atomic coordinates (× 10^4) for **3**

Atom	*x*	*y*	*z*
Au(1)	10 754.8(8)	1 439.1(2)	7 384.1(6)
Au(2)	8 721.6(7)	1 124.2(2)	5 964.2(6)
Au(3)	8 608.1(8)	1 066.4(2)	3 840.0(7)
Rh	7 289(1)	1 872(1)	4 207(1)
Ru(1)	10 535(1)	1 361(1)	5 188(1)
Ru(2)	9 071(1)	1 860(1)	6 043(1)
Ru(3)	9 602(1)	1 976(1)	4 126(1)
Fe	9 902(2)	705(1)	9 304(2)
P(1)	11 904(3)	1 275(1)	9 015(3)
P(2)	7 966(3)	716(1)	6 795(3)
Cl	7 742(5)	689(2)	2 489(5)
O(1)	11 582(11)	680(3)	6 152(11)
O(2)	12 720(10)	1 778(3)	6 340(10)
O(3)	11 500(14)	1 263(4)	3 392(12)
O(4)	7 386(10)	1 701(3)	7 228(9)
O(5)	10 755(12)	2 307(3)	7 706(10)
O(6)	8 421(12)	2 662(3)	3 460(12)
O(7)	9 012(13)	1 713(4)	1 874(10)
O(8)	12 098(11)	2 227(4)	4 341(11)
O(9)	7 599(11)	2 496(3)	5 517(9)
B	8 669(15)	1 554(4)	4 615(12)
C(1)	11 163(16)	931(5)	5 848(13)
C(2)	11 891(15)	1 634(5)	5 939(13)
C(3)	11 127(16)	1 299(5)	4 041(14)
C(4)	8 063(13)	1 741(4)	6 828(12)
C(5)	10 108(17)	2 135(5)	7 120(13)
C(6)	8 805(16)	2 394(5)	3 696(12)
C(7)	9 220(15)	1 804(5)	2 708(15)
C(8)	11 174(15)	2 127(5)	4 287(13)
C(9)	7 861(14)	2 222(4)	5 371(12)
C(11)	5 713(13)	1 539(5)	3 486(14)
C(12)	5 994(15)	1 741(7)	2 690(13)
C(13)	5 835(16)	2 088(6)	2 837(15)
C(14)	5 458(15)	2 117(5)	3 691(14)
C(15)	5 414(15)	1 792(5)	4 112(13)
C(16)	5 543(17)	1 162(5)	3 499(20)
C(17)	6 148(19)	1 581(8)	1 735(16)
C(18)	5 876(22)	2 358(8)	2 082(20)
C(19)	5 022(19)	2 443(5)	4 030(22)
C(20)	4 979(21)	1 703(8)	5 015(19)
C(21)	8 548(15)	714(5)	9 922(13)
C(22)	8 154(14)	550(4)	8 932(12)
C(23)	8 295(12)	779(3)	8 183(11)
C(24)	8 771(13)	1 098(4)	8 717(11)
C(25)	8 913(15)	1 055(4)	9 778(11)
C(26)	11 167(14)	383(4)	10 217(15)
C(27)	10 921(16)	297(4)	9 181(15)
C(28)	11 176(12)	580(4)	8 634(12)
C(29)	11 532(13)	854(4)	9 378(12)
C(30)	11 558(14)	737(5)	10 349(13)
C(31)	12 728(14)	1 550(5)	11 023(13)
C(32)	12 665(17)	1 748(5)	11 783(13)
C(33)	11 771(18)	1 997(5)	11 621(15)
C(34)	10 882(18)	1 996(5)	10 689(14)
C(35)	10 938(17)	1 785(4)	9 886(13)
C(36)	11 857(13)	1 558(4)	10 073(11)
C(41)	13 955(15)	1 535(5)	8 792(14)
C(42)	15 137(17)	1 532(6)	8 829(16)
C(43)	15 838(17)	1 263(7)	9 236(17)
C(44)	15 390(18)	993(7)	9 566(17)
C(45)	14 188(16)	982(5)	9 517(16)
C(46)	13 468(13)	1 263(4)	9 127(12)
C(51)	9 329(15)	210(4)	6 306(14)
C(52)	9 722(18)	−99(5)	6 294(17)
C(53)	9 259(18)	−364(5)	6 670(15)
C(54)	8 306(16)	−312(4)	6 962(15)
C(55)	7 878(14)	11(4)	6 988(12)
C(56)	8 417(14)	277(4)	6 674(12)
C(61)	5 661(14)	869(5)	6 725(13)
C(62)	4 433(17)	864(6)	6 301(15)
C(63)	3 930(16)	671(6)	5 420(17)
C(64)	4 614(16)	486(5)	4 984(16)
C(65)	5 850(14)	504(4)	5 398(13)
C(66)	6 365(12)	689(4)	6 293(12)
C(101)	3 849(59)	135(18)	8 393(52)
C(102)	3 889(54)	193(16)	7 948(48)
C(103)	4 489(50)	−30(15)	7 610(44)
C(104)	5 738(22)	−318(7)	8 265(22)
C(105)	5 369(51)	−312(15)	7 833(44)
C(106)	5 772(34)	−184(11)	8 629(31)

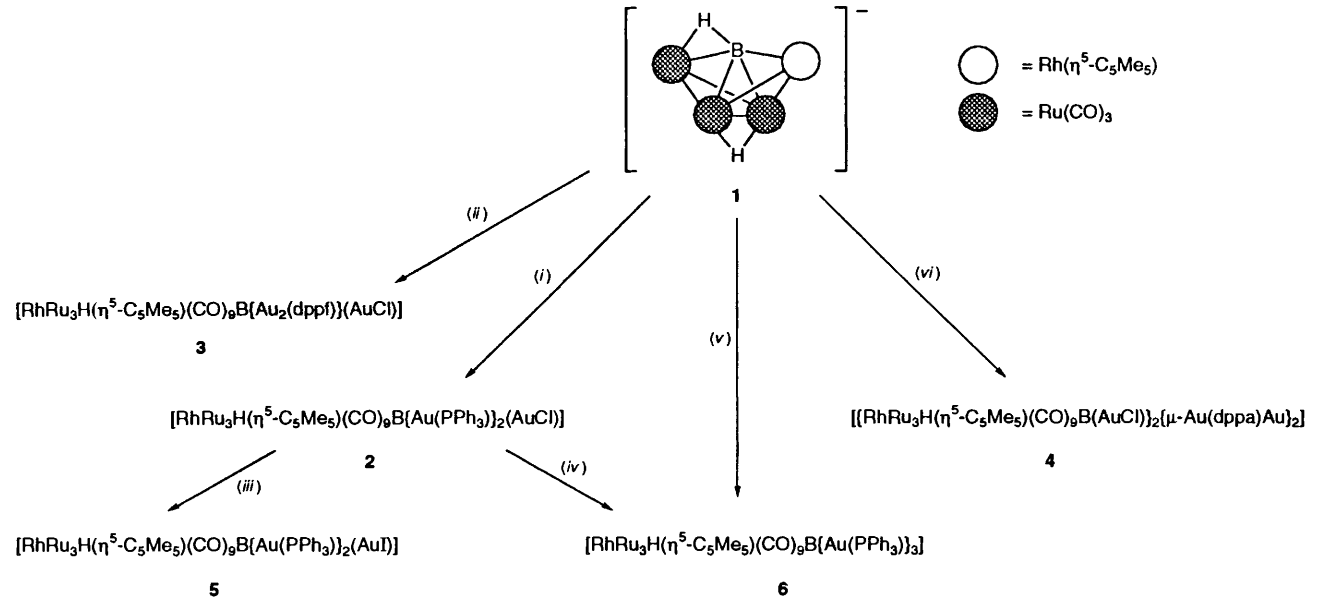

Scheme 1 (*i*) [AuCl(PPh$_3$)]; (*ii*) [Au$_2$Cl$_2$(dppf)]; (*iii*) [NEt$_4$]I; (*iv*) Tl[PF$_6$] or [N(PPh$_3$)$_2$]Cl, and PPh$_3$; (*v*) [{Au(PPh$_3$)}$_3$O][BF$_4$]; (*vi*) [Au$_2$Cl$_2$(dppa)]

observed in one of two isomers of [Ru$_4$H(CO)$_{12}$B{Au[P(C$_6$H$_4$Me-2)$_3$]}$_2$].[5]

The most interesting, and indeed unusual, feature in the structure of **2** is the presence of a {AuCl} unit which bridges the edge Ru(2)–B. The gold atom of this unit is within bonding distance of atom Au(2) [Au(2)–Au(3) 2.831(2) Å], producing a

V-shaped array of gold atoms [Au(1)–Au(2)–Au(3) 114.3(1)°] which, overall, is associated with the boron atom and two of the ruthenium atoms. The unit is skewed away from the wing-tip-rhodium atom and lies towards the hinge atoms of the butterfly. Fig. 3 illustrates the {RhRu$_3$BAu$_3$} core of **2**. Its geometry is quite different from that of the core of [Fe$_4$(CO)$_{12}$B-{Au(PPh$_3$)}$_3$][8] shown in Fig. 1(*a*). A factor contributing to this difference may be that the C$_5$Me$_5$ ring in **2** is oriented so as effectively to block the Rh–B site from being bridged by a gold(I) phosphine unit.

Whilst the Au(2)–B distance is typical of other gold(phosphine)–boron bond lengths observed in related clusters,[17] the Au(3)–B distance is significantly shorter; Au(2)–B 2.35(3), Au(3)–B 2.18(3) Å. These differences are consistent with observations made[18] for a series of centred gold clusters in which distances from the central atom (in our case the boron atom) to the peripheral gold atoms are smaller for the less sterically demanding AuCl group than for AuL (L = phosphine) units. Further comment on the inclusion of the {AuCl} unit is given after the discussion of the structure of compound **3**.

As mentioned above, the ^{1}H NMR spectrum of **2** displays a high-field singlet which indicates the presence of a cluster-bound hydrogen atom. This atom was not located directly by X-ray structural analysis. However, inspection of the orientation of the carbonyl ligands, and the fact that the singlet nature of the NMR spectral signal shows that there is no direct Rh–H interaction, lead us to conclude that the hydrogen atom bridges the edge Ru(1)–Ru(3).

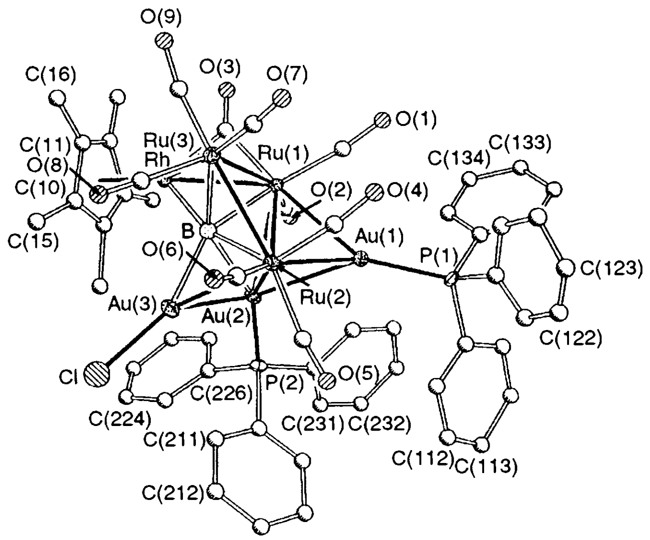

Fig. 2 Molecular structure of **2**. The cluster hydrogen atom is not shown

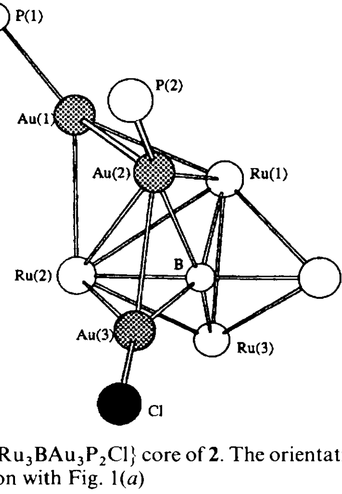

Fig. 3 The {RhRu$_3$BAu$_3$P$_2$Cl} core of **2**. The orientation of this figure allows comparison with Fig. 1(*a*)

Crystal Structure of [RhRu$_3$H(η^5-C$_5$Me$_5$)(CO)$_9$B{Au$_2$(dppf)}(AuCl)]·CH$_2$Cl$_2$ **3**·CH$_2$Cl$_2$.—X-Ray quality crystals of **3**·CH$_2$Cl$_2$ were grown at −25 °C from a concentrated CH$_2$Cl$_2$ solution layered with hexane. The molecular structure of **3** is shown in Fig. 4; selected bond distances and angles in Table 5.

Table 4 Selected bond distances (Å) and angles (°) for **2** *

Au(1)–Au(2)	2.923(2)	Au(1)–Ru(1)	2.794(2)
Au(1)–Ru(2)	2.856(3)	Au(1)–P(1)	2.297(6)
Au(2)–Au(3)	2.831(2)	Au(2)–P(2)	2.289(7)
Au(2)–Ru(1)	2.849(2)	Au(2)–Ru(2)	2.897(3)
Au(3)–Ru(2)	2.682(2)	Au(3)–Cl	2.319(8)
Au(2)–B	2.35(3)	Au(3)–B	2.18(3)
Rh–Ru(1)	2.717(3)	Rh–Ru(3)	2.827(3)
Ru(1)–Ru(2)	3.095(3)	Ru(1)–Ru(3)	2.901(3)
Ru(2)–Ru(3)	2.868(3)	Ru(1)–B	2.25(3)
Ru(2)–B	2.20(3)	Ru(3)–B	2.23(3)
Rh–B	2.03(3)	Rh–cp	1.90(1)
Au(2)–Au(1)–Ru(1)	59.7(1)	Au(2)–Au(1)–Ru(2)	60.2(1)
Ru(1)–Au(1)–Ru(2)	66.4(1)	Au(2)–Au(1)–P(1)	140.1(2)
Ru(1)–Au(1)–P(1)	145.5(2)	Ru(2)–Au(1)–P(1)	143.5(2)
Au(1)–Au(2)–Au(3)	114.3(1)	Au(1)–Au(2)–Ru(1)	57.9(1)
Au(3)–Au(2)–Ru(1)	98.0(1)	Au(1)–Au(2)–Ru(2)	58.8(1)
Au(3)–Au(2)–Ru(2)	55.8(1)	Ru(1)–Au(2)–Ru(2)	65.2(1)
Au(1)–Au(2)–P(2)	112.7(1)	Au(3)–Au(2)–P(2)	114.2(2)
Ru(1)–Au(2)–P(2)	146.3(2)	Ru(2)–Au(2)–P(2)	142.0(2)
Au(1)–Au(2)–B	90.5(6)	Au(3)–Au(2)–B	48.6(6)
Ru(1)–Au(2)–B	50.1(6)	Ru(2)–Au(2)–B	48.1(7)
P(2)–Au(2)–B	156.6(6)	Au(2)–Au(3)–Ru(2)	63.3(1)
Au(2)–Au(3)–Cl	132.7(2)	Ru(2)–Au(3)–Cl	149.7(2)
Au(2)–Au(3)–B	53.9(7)	Ru(2)–Au(3)–B	52.5(7)
Cl–Au(3)–B	156.2(6)	Au(2)–B–Au(3)	77.4(8)
Au(2)–B–Rh	111.3(14)	Au(3)–B–Rh	121.8(11)
Au(2)–B–Ru(1)	76.7(9)	Au(3)–B–Ru(1)	151.7(12)
Rh–B–Ru(1)	78.7(9)	Au(2)–B–Ru(2)	79.2(8)
Au(3)–B–Ru(2)	75.7(9)	Rh–B–Ru(2)	160.6(14)
Ru(1)–B–Ru(2)	88.4(8)	Au(2)–B–Ru(3)	150.0(11)
Au(3)–B–Ru(3)	118.5(14)	Rh–B–Ru(3)	82.9(9)
Ru(1)–B–Ru(3)	80.7(8)	Ru(2)–B–Ru(3)	80.7(10)

* cp = C$_5$Me$_5$ Ring centroid.

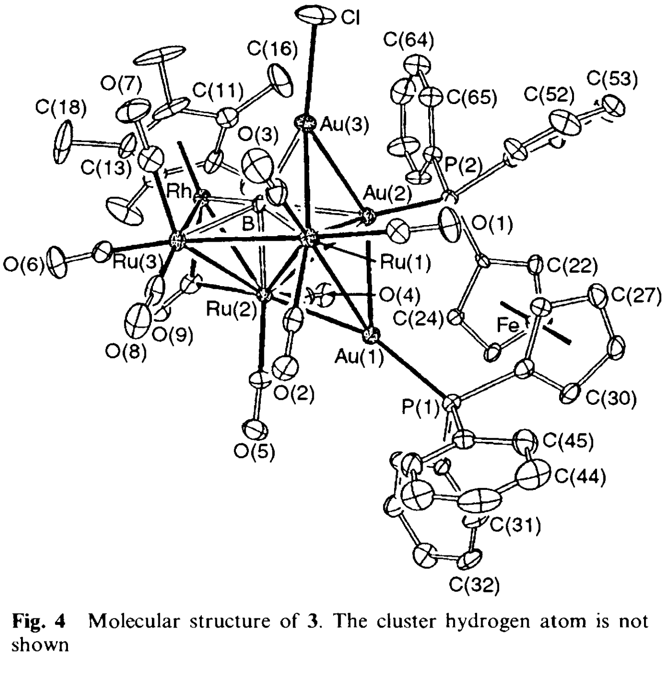

Fig. 4 Molecular structure of **3**. The cluster hydrogen atom is not shown

Table 5 Selected bond distances (Å) and angles (°) for **3***

Au(1)–Au(2)	2.850(1)	Au(1)–Ru(1)	2.913(2)
Au(1)–Ru(2)	2.781(1)	Au(1)–P(1)	2.286(4)
Au(2)–Au(3)	2.840(1)	Au(2)–P(2)	2.303(4)
Au(2)–Ru(1)	2.843(2)	Au(2)–Ru(2)	2.922(1)
Au(3)–Ru(1)	2.695(1)	Au(3)–Cl	2.324(6)
Au(2)–B	2.47(2)	Au(3)–B	2.18(2)
Rh–Ru(2)	2.704(2)	Rh–Ru(3)	2.823(2)
Ru(1)–Ru(2)	3.085(2)	Ru(1)–Ru(3)	2.853(2)
Ru(2)–Ru(3)	2.894(2)	Ru(1)–B	2.24(2)
Ru(2)–B	2.19(2)	Ru(3)–B	2.21(2)
Rh–B	2.00(2)	Rh–cp^1	1.90(1)
Fe–cp^2	1.65(1)		
Fe–cp^3	1.64(1)		

Au(2)–Au(1)–Ru(1)	59.1(1)	Au(2)–Au(1)–Ru(2)	62.5(1)
Ru(1)–Au(1)–Ru(2)	65.6(1)	Au(2)–Au(1)–P(1)	130.2(1)
Ru(1)–Au(1)–P(1)	141.7(1)	Ru(2)–Au(1)–P(1)	152.0(1)
Au(1)–Au(2)–Au(3)	118.2(1)	Au(1)–Au(2)–Ru(1)	61.5(1)
Au(3)–Au(2)–Ru(1)	56.6(1)	Au(1)–Au(2)–Ru(2)	57.6(1)
Au(3)–Au(2)–Ru(2)	94.4(1)	Ru(1)–Au(2)–Ru(2)	64.7(1)
Au(1)–Au(2)–P(2)	110.8(1)	Au(3)–Au(2)–P(2)	122.5(1)
Ru(1)–Au(2)–P(2)	150.5(1)	Ru(2)–Au(2)–P(2)	138.3(1)
Au(1)–Au(2)–B	90.9(4)	Au(3)–Au(2)–B	47.8(4)
Ru(1)–Au(2)–B	49.3(4)	Ru(2)–Au(2)–B	47.1(4)
P(2)–Au(2)–B	156.2(4)	Au(2)–Au(3)–Ru(1)	61.7(1)
Au(2)–Au(3)–Cl	135.4(2)	Ru(1)–Au(3)–Cl	151.0(2)
Au(2)–Au(3)–B	57.3(5)	Ru(1)–Au(3)–B	53.5(4)
Cl–Au(3)–B	151.6(4)	Au(2)–B–Au(3)	75.0(5)
Au(2)–B–Rh	117.2(9)	Au(3)–B–Rh	121.4(7)
Au(2)–B–Ru(1)	74.0(5)	Au(3)–B–Ru(1)	75.2(6)
Rh–B–Ru(1)	161.0(9)	Au(2)–B–Ru(2)	77.3(5)
Au(3)–B–Ru(2)	150.6(8)	Rh–B–Ru(2)	80.1(7)
Ru(1)–B–Ru(2)	88.2(5)	Au(2)–B–Ru(3)	146.8(7)
Au(3)–B–Ru(3)	117.4(9)	Rh–B–Ru(3)	84.0(6)
Ru(1)–B–Ru(3)	79.6(6)	Ru(2)–B–Ru(3)	82.1(6)
cp^1–Fe–cp^2	177.7(7)		

* cp^1 = C_5Me_5 Ring centroid, cp^2 = C(21)–C(25) centroid, cp^3 = C(26)–C(30) centroid.

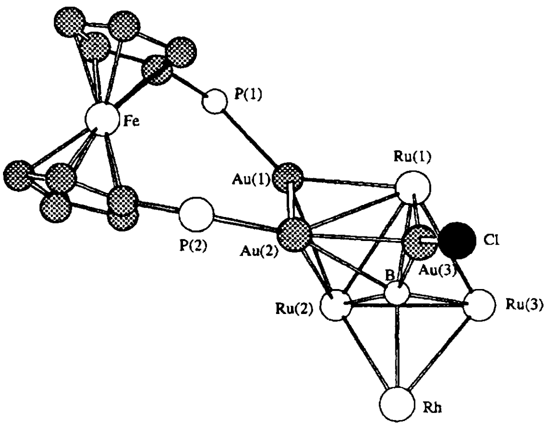

Fig. 5 Structure of the core of 3

The molecular structure of **3** is closely related to that of **2**, and the detailed geometry of the core of **3** (Fig. 5) is very similar to that of **2**. The {Au_2(dppf)} moiety bridges across one side of the butterfly framework, and the presence of the dppf ligand in place of two PPh_3 ligands produces little structural perturbation of the cluster core in going from **2** to **3**. The two cyclopentadienyl rings of the dppf ligand are mutually twisted by ≈ 14° making the orientation of the ferrocene unit part-way between being eclipsed and staggered. The cyclopentadienyl rings are mutually oriented such that the C–P bonds diverge from one another. This arrangement is quite similar to that observed in [$Ru_4H(CO)_{12}B\{Au_2$(dppf)}], although here the {Au_2(dppf)} unit was symmetrically bound to the {$Ru_4H(CO)_{12}B$}-cluster core.[6]

As in **2**, a gold(I) chloride unit {Au(3)Cl} is incorporated into cluster **3**, and bridges the edge Ru(1)–B. [This corresponds to the edge Ru(2)–B in compound **2**.] The three gold centres form a V-shaped unit with an angle Au(1)–Au(2)–Au(3) of 118.2(1)°, which is slightly larger than the corresponding angle in compound **2**. The two gold–boron distances are 2.18(2) for the {AuCl} unit, and 2.47(2) Å for the gold phosphine unit. As in **2**, the pattern is for a shorter interaction with the less bulky {AuCl} unit.[18] The distances Au(1)–Au(2) and Au(2)–Au(3) are 2.850(1) and 2.840(1) Å respectively, and are both indicative of gold–gold bonding interactions.

The cluster-bound hydrogen atom in **3** was not located directly, but using a similar argument to that described above for compound **2**, we propose that this H atom bridges the edge Ru(2)–Ru(3).

Comments on the Presence of the Gold(I) *Chloride Unit.*—Gold halide units are known to be features of clusters involving some later transition metals. For example, clusters such as [$Au_{10}Cl_3\{P(C_6H_{11})_2Ph\}_6]^{3+}$ incorporate both {AuCl}- and {$Au(PR_3)$}-fragments.[18–20] Examples of gold–platinum clusters containing the {AuCl} motif have also been reported.[21] Mingos and co-workers[19,20,22] have shown that radial bonding interactions which involve the gold sp hybrid orbitals are crucially important in Au_x clusters. The electrons in the filled 5d shell make little contribution to the cluster bonding.

The inclusion of a {AuCl} fragment in a metal carbonyl cluster is unusual. A relatively unstable osmium carbide cluster possessing a face-capping {AuBr} unit, [$Os_{10}C(CO)_{24}(AuBr)]^{2-}$, has been prepared from the reaction of [$Os_{10}C(CO)_{24}]^{2-}$ with [$AuBr(PPh_3)$] and structurally characterised.[23] The anion [$Os_{10}C(CO)_{24}(AuBr)]^{2-}$ is paramagnetic and displays an ESR signal consistent with the gold atom being formally assigned as an Au^{II} centre. There is no evidence that either **2** or **3** is paramagnetic, and we assign each of the three gold centres in these two compounds as being in an oxidation state of + 1. A consideration of the electron count in clusters **2** and **3** is also consistent with these assignments. In transition-metal clusters containing gold fragments which are bound to the extremities of the cluster (usually in edge-bridging or face-capping modes), the gold atoms are not generally considered to be cluster vertices and the cluster electron count is totalled by considering (for example) a {$Au(PPh_3)$} unit to contribute just one electron. Thus, we would expect each of compounds **2** and **3** to possess valence electron counts that are consistent with a butterfly skeleton. A 62-electron count for compound **2** can be achieved if each {$Ru(CO)_3$} and {$Rh(\eta^5\text{-}C_5Me_5)$} unit contributes 14 electrons, the boron atom three electrons, each {$Au(PPh_3)$} unit one electron, the cluster-bound hydrogen atom one electron, and the {AuCl} unit zero electrons. These counts for the gold-containing fragments follow from an assumption of the presence of three gold(I) centres. An analogous argument can be applied to compound **3**.

The zero-electron {Au^ICl} moiety seemingly has little to contribute towards the bonding in the cluster other than supplementary Au ··· Au interactions. The aggregation of gold fragments on the surface of transition-metal carbonyl clusters is not a new feature[1,2,3,8] but for the most part such fragments are gold(I) phosphines originating from the reactions of transition-metal carbonyl cluster anions with gold(I) phosphine halides. In our own work, we have used this strategy on a number of occasions and have not previously observed the inclusion of a gold(I) *halide* unit in a cluster product. Compounds **2** and **3** may, perhaps, be regarded as donor–acceptor complexes in which the [$RhRu_3H(\eta^5\text{-}C_5Me_5)(CO)_9B(Au_2L_2)$] (L = PPh_3 or L_2 = dppf) cluster functions as an electron donor to the gold(I) chloride moiety. The formation of peripheral Au ··· Au interactions may encourage the formation of **2** and **3**.

Comparisons with previous results[6,17] involving closely related tetraruthenium boron-containing butterfly systems suggest that products of the type $[RhRu_3H(\eta^5\text{-}C_5Me_5)(CO)_9B(Au_2L_2)]$ ($L = PPh_3$ or L_2 = dppf) should be formed. However, such neutral systems could not be isolated and we consistently observe **2** and **3** as the predominant products.

Reactivity of Cluster **2**.—As representative of both clusters **2** and **3**, we have studied the reactivity of compound **2**, with particular emphasis on the behaviour of the {AuCl} unit (Scheme 1). Compound **2** reacts readily with tetraethylammonium iodide to give $[RhRu_3H(\eta^5\text{-}C_5Me_5)(CO)_9B\{Au(PPh_3)\}_2(AuI)]$ **5**, typically in ≈80% yield. The product exhibits a parent ion at *m/z* 2048 in its FIB mass spectrum which is consistent with simple iodide-for-chloride exchange. This exchange produces little or no perturbation to the IR, and ^1H and ^{11}B NMR spectroscopic signatures of the cluster on going from **2** to **5**, suggesting that no gross structural changes have accompanied the reaction. The only noticeable difference is a small shift in the resonance assigned to the Ru–H–Ru bridging hydrogen atom from δ −18.86 (**2**) to − 18.77 (**5**) in the ^1H NMR spectrum. This change is not regarded as being of significance. The preference of gold for iodide rather than chloride contacts may be rationalised on the basis of soft–soft interactions; the iodine 5s–5p is better matched in energy terms with the $6s\text{–}6p_z$ hybrid orbital of the gold atom than is the chlorine 3s–3p orbitals.

When gold(I) phosphine derivatives of transition-metal carbonyl clusters are prepared, the principle is generally to replace a cluster-bound hydrogen atom by the gold(I) phosphine fragment. This may take place in two steps {deprotonation followed by reaction with a source of $[Au(PR_3)]^+$}. Alternatively, the replacement may occur spontaneously without the need for a formal deprotonation step. In earlier work, we have observed that mono-, di- *and* tri-[gold(I) phosphine] derivatives can be formed from the anion $[Fe_4H(CO)_{12}BH]^-$.[3] However, when the precursor is $[Ru_4H(CO)_{12}BH]^-$, only mono- and di-[gold(I) phosphine] derivatives have been isolated.[3,5] The formations of mono-cluster products compete with cluster-fusion processes which involve Au–P bond cleavage.[5] The inclusion of *three* gold atoms in **2**, **3** and **5** therefore intrigued us. Further, we wondered why the presence of a {AuX} unit (X = Cl or I) with the associated retention of a cluster-bound hydrogen atom was preferred to hydrogen abstraction and the addition of a $\{Au(PR_3)\}$ unit. The question of steric control appeared to be a plausible contributing factor.

In order to investigate this aspect of the chemistry, we treated compound **2** with PPh_3 in the presence of $Tl[PF_6]$, the aim being to abstract the chloride ion and encourage the *in situ* formation of a third $\{Au(PPh_3)\}$ unit. A brown compound **6** was isolated in high yield. The most noticeable feature in the ^1H NMR spectrum of compound **6** was the absence of a signal in the high-field region, and this indicated that the Ru–H–Ru bridging hydrogen atom had been removed during the conversion from **2** to **6**. The ^{11}B NMR spectrum of compound **6** displays a broad resonance at δ +167; this is shifted downfield with respect to the signal for compound **2** by 9 ppm. A single resonance at δ +53.5 was observed in the ^{31}P NMR spectrum of **6**, which contrasted with the presence of two equal intensity signals (δ +43.4 and +57.5) observed in the spectrum of compound **2**. The FAB mass spectrum of product **6** showed a parent ion at *m/z* 2183. An envelope centred at 1724 was consistent with the loss of one $\{Au(PPh_3)\}$ fragment. These mass spectral data, and the isotopic distribution pattern of the parent-ion envelope, are consistent with a formulation for **6** of $[RhRu_3(\eta^5\text{-}C_5Me_5)(CO)_9B\{Au(PPh_3)\}_3]$. The ^{31}P NMR spectral data indicate that, unlike **2**, compound **6** is fluxional in solution; given the low symmetry of the $RhRu_3B$-butterfly framework it seems unlikely that the three $\{Au(PPh_3)\}$ units can be equivalent in a static model. We have previously observed that the trigold derivative $[Fe_4(CO)_{12}B\{Au(PPh_3)\}_3]$ remains fluxional at low temperatures.[8] The tri(gold phosphine) derivative **6** can also be prepared in ≈70% yield by treating **2** with $[N(PPh_3)_2]Cl$ and PPh_3.

Reaction of $[N(PPh_3)_2][RhRu_3H(\eta^5\text{-}C_5Me_5)(CO)_9BH]$ *with* $[\{Au(PPh_3)\}_3O][BF_4]$.—Since the tri[gold(I) phosphine] derivative $[RhRu_3(\eta^5\text{-}C_5Me_5)(CO)_9B\{Au(PPh_3)\}_3]$ **6** can indeed be prepared and does not appear to be sterically hindered, we returned to the question of its direct synthesis from the anion $[RhRu_3H(\eta^5\text{-}C_5Me_5)(CO)_9BH]^-$ **1**. The oxonium ion $[\{Au(PPh_3)\}_3O]^+$ is a useful reagent for simultaneously introducing three gold(I) phosphine units into a cluster,[1b,8,24] and the reaction of $[\{Au(PPh_3)\}_3O][BF_4]$ with the $[N(PPh_3)_2]^+$ salt of **1** leads to the formation of compound **6** in ≈40% yield. Interestingly, compound **2** is also formed (25% yield), and this observation raises a question as regards the source of the chloride ligand. There appear to be two possibilities. First, the solvent is dichloromethane. Secondly, the formation of the precursor **1** involves the use of $[N(PPh_3)_2]Cl$ and it is possible that not all of this had been removed from the sample of $[N(PPh_3)_2][RhRu_3H(\eta^5\text{-}C_5Me_5)(CO)_9BH]$.

A third product **7** was also obtained from the reaction of anion **1** with $[\{Au(PPh_3)\}_3O]^+$. The FAB mass spectrum of compound **7** exhibits a parent ion at *m/z* 1266 which corresponds to a formulation of $[RhRu_3H_2(\eta^5\text{-}C_5Me_5)(CO)_9B\{Au(PPh_3)\}]$, and indicates that **7** is formed by the simple addition of one $\{Au(PPh_3)\}$ unit to anion **1**. The high-field region of the ^1H NMR spectrum exhibits two signals of equal intensity at δ −14.5 and −20.4, the shifts of which are typical of metal–metal edge-bridging hydrogen atoms. These signals are slightly broadened, suggesting the onset of a fluxional process. In going from **1** to **7**, the hydrogen atom which bridged a metal–boron edge in **1** has migrated on to the metal-butterfly framework. This may provide indirect evidence that both the hydrogen atom and gold(I) unit compete for the same site. If the pattern that is seen in compounds **2** and **3** is followed in **7**, then the gold(I) unit should show a preference for association with a ruthenium rather than rhodium atom. We therefore propose that the $\{Au(PPh_3)\}$ unit bridges the $Ru_{wing\text{-}tip}\text{–}B$ edge, although we cannot rule out the possibility of a face-capping position. It follows that in **1**, the bridging hydrogen atom may occupy an $Ru_{wing\text{-}tip}\text{–}B$ bridging site in preference to a $Rh_{wing\text{-}tip}\text{–}B$ bridging position. Addition of the gold fragment causes a rearrangement of this hydrogen atom. Since no $^{103}Rh\text{–}^1H$ spin–spin coupling is observed in either of the high-field proton signals in the spectrum of **7**, we propose that both occupy Ru–Ru bridging sites. The signal at δ −20.4 is consistent with the retention of one hydrogen atom bridging the $Ru_{hinge}\text{–}Ru_{hinge}$ edge, whilst the signal at δ −14.5 is indicative of an $Ru_{wing\text{-}tip}\text{–}H\text{–}Ru_{hinge}$ bridging interaction. Very similar shifts (δ −20.55 and −14.41) are observed for the $Ru_{hinge}\text{–}H\text{–}Ru_{hinge}$ and $Ru_{wing\text{-}tip}\text{–}H\text{–}Ru_{hinge}$ bridging protons in the related cluster $[RhRu_3H_2(\eta^5\text{-}C_5Me_5)(CO)_8(PPh_3)BH]$.[9]

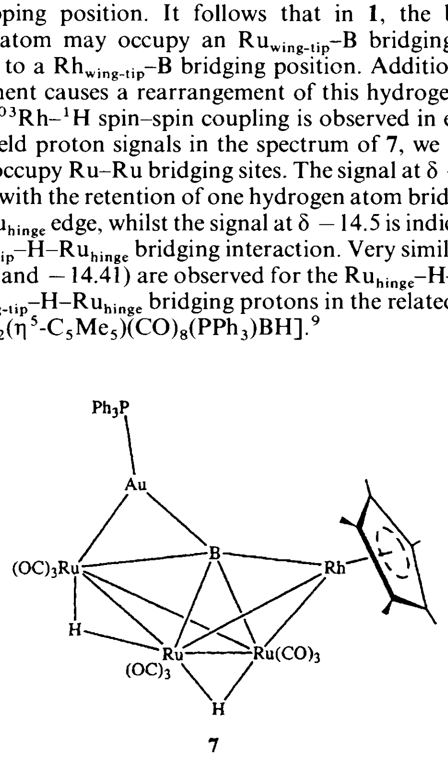

7

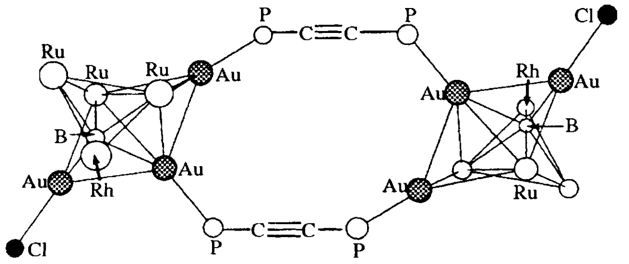

4 Ru = $Ru(CO)_3$
Rh = $(\eta^5\text{-}C_5Me_5)$
P = PPh_2

A significant downfield shift in the ^{11}B NMR spectroscopic signal from δ +149 (in **1**) to δ +174 (in **7**) is indicative of an increase in the degree of direct metal-to-boron bonding. This is consistent with the addition of the gold(I) fragment and associated proton migration described above.

Reaction of **1** *with* $[Au_2Cl_2(dppa)]$.—The dppa ligand possesses a rigid acetylenic backbone and has previously been used to link cluster units.[25,26] The digold derivative of this ligand $[Au_2Cl_2(dppa)]$ has been used by Lewis and co-workers[25] as a potential source of a cluster linkage, namely a {Au(dppa)Au} unit. Interestingly in this case however, the product proved to be $[\{Os_4H(CO)_{12}\}_2\{\mu\text{-Au(dppa)}\}_2]$ rather than the expected $[\{Os_4H_2(CO)_{12}\}_2\{\mu\text{-Au(dppa)Au}\}_2]$, although the reaction was carried out at an elevated temperature.

The reaction of anion **1** with $[Au_2Cl_2(dppa)]$ generates one major product, compound **4**. The parent ion in the mass spectrum of this product (*m/z* 3654) is consistent with **4** being formulated as the linked-cluster $[\{RhRu_3H(\eta^5\text{-}C_5Me_5)(CO)_9B(AuCl)\}_2\{\mu\text{-Au(dppa)Au}\}_2]$. The solution spectroscopic characteristics of compound **4** compare favourably with those of compounds **2** and **3**. The values and pattern of the infrared absorptions of the three compounds are strikingly similar (**4**, ν_{CO} 2059s, 2029s, 2000vs, 1947w, 1791w cm^{-1}; **2**, ν_{CO} 2058vs, 2026m, 2000vs, 1969w (sh), 1944w, 1788w cm^{-1}; **3**, ν_{CO} 2058vs, 2025m, 1999vs, 1966w (sh), 1942w, 1785w cm^{-1}) suggesting structural similarities. Crystallographic evidence has already confirmed the close relationship between compounds **2** and **3**. The ^{11}B NMR spectral resonance for **4** is δ +159 compared with a value of δ +158 for both **2** and **3**. In addition to signals attributed to the methyl (C_5Me_5) and phenyl (PPh_2) protons, the ^1H NMR spectrum shows a highfield singlet at δ −19.19, indicative of a Ru–H–Ru bridging proton, and close in shift to corresponding signals for compounds **2** and **3**. The ^{31}P NMR spectrum of compound **4** exhibits two singlets (1:1); a similar pattern is observed for **2** and **3**. These data permit us to propose a structure for **4** in which two $\{RhRu_3H(\eta^5\text{-}C_5Me_5)(CO)_9B(AuCl)\}$ subclusters are linked by two {Au(dppa)Au} bridges. The data are in accord with each subcluster possessing a structure analogous to those of compounds **2** and **3**.

Acknowledgements

We thank the donors of the Petroleum Research Fund, administered by the American Chemical Society for support of this work (grant 25533-AC3), to the SERC for a studentship (to J. R. G.) and to the National Science Foundation for a grant (CHE 9007852) towards the purchase of a diffractometer at the University of Delaware.

References

1 See, for example, (*a*) J. W. Lauher and K. Wald, *J. Am. Chem. Soc.*, 1981, **103**, 7648; (*b*) I. D. Salter, *Adv. Organomet. Chem.*, 1989, **29**, 249.
2 D. L. Sunick, P. S. White and C. K. Schauer, *Angew. Chem., Int. Ed. Engl.*, 1994, **33**, 75.
3 C. E. Housecroft, *Adv. Organomet. Chem.*, 1991, **33**, 1 and refs. therein.
4 C. E. Housecroft, M. S. Shongwe, A. L. Rheingold and P. J. Zanello, *J. Organomet. Chem.*, 1991, **408**, 7.
5 S. M. Draper, C. E. Housecroft, J. E. Rees, M. S. Shongwe, B. S. Haggerty and A. L. Rheingold, *Organometallics*, 1992, **11**, 2356.
6 S. M. Draper, C. E. Housecroft and A. L. Rheingold, *J. Organomet. Chem.*, 1992, **435**, 9.
7 A. G. Cowie, B. F. G. Johnson, J. Lewis and P. R. Raithby, *J. Chem. Soc., Chem. Commun.*, 1984, 1710.
8 K. S. Harpp, C. E. Housecroft, A. L. Rheingold and M. S. Shongwe, *J. Chem. Soc., Chem. Commun.*, 1988, 965.
9 J. R. Galsworthy, C. E. Housecroft, D. M. Matthews, R. Ostrander and A. L. Rheingold, *J. Chem. Soc., Dalton Trans.*, 1994, 69.
10 F. G. Mann, A. F. Wells and D. J. Purdie, *J. Chem. Soc.*, 1937, 1828.
11 D. R. Williamson and M. C. Baird, *J. Inorg. Nucl. Chem.*, 1972, **34**, 3393.
12 D. T. Hill, G. R. Girard, F. L. McCabe, R. K. Johnson, P. D. Stupik, J. H. Zhang, W. M. Reiff and D. S. Eggleston, *Inorg. Chem.*, 1989, **28**, 3529; A. Houlton, R. M. G. Roberts, J. Silver and R. V. Parish, *J. Organomet. Chem.*, 1991, **418**, 269.
13 A. J. Carty and A. Efraty, *Inorg. Chem.*, 1969, **8**, 543.
14 A. N. Nesmeyanov, E. G. Perevalova, Yu. T. Struchkov, M. Yu. Antipin, K. I. Grandberg and V. P. Dyadchenko, *J. Organomet. Chem.*, 1980, **201**, 343.
15 G. Sheldrick, SHELXTL-PC software version 4.2, Siemens XRD, Madison, WI, USA, 1990.
16 See, for example, N. P. Rath and T. P. Fehlner, *J. Am. Chem. Soc.*, 1988, **110**, 5345.
17 A. K. Chipperfield and C. E. Housecroft, *Organometallics*, 1990, **9**, 681.
18 See, for example, C. E. Briant, B. R. C. Theobald, J. W. White, L. K. Bell, D. M. P. Mingos and A. J. Welch, *J. Chem. Soc., Chem. Commun.*, 1981, 201; C. E. Briant, K. P. Hall, A. C. Wheeler and D. M. P. Mingos, *J. Chem. Soc., Chem. Commun.*, 1984, 248; S. G. Bott, H. Fleischer, M. Leach, D. M. P. Mingos, H. Powell, D. J. Watkin and M. J. Watson, *J. Chem. Soc., Dalton Trans.*, 1991, 2569.
19 D. M. P. Mingos, *J. Chem. Soc., Dalton Trans.*, 1976, 1163.
20 K. P. Hall and D. M. P. Mingos, *Prog. Inorg. Chem.*, 1984, **32**, 237.
21 M. F. J. Schoondergang, J. J. Boer, G. P. F. Strijdonck, P. P. J. Schlebos, W. P. Bosman, J. M. M. Smits, P. T. Beurskens and J. J. Steggerda, *Inorg. Chem.*, 1991, **30**, 2048.
22 D. M. P. Mingos and D. J. Wales, *Introduction to Cluster Chemistry*, Prentice Hall, New Jersey, 1990.
23 S. R. Drake, K. Henrick, B. F. G. Johnson, J. Lewis, M. McPartlin and J. Morris, *J. Chem. Soc., Chem. Commun.*, 1986, 928.
24 See, for example, L. W. Bateman, M. Green, K. A. Mead, R. M. Mills, I. D. Salter, F. G. A. Stone and P. Woodward, *J. Chem. Soc., Dalton Trans.*, 1983, 2599; L. W. Bateman, M. Green, J. A. K. Howard, K. A. Mead, R. M. Mills, I. D. Salter, F. G. A. Stone and P. Woodward, *J. Chem. Soc., Chem. Commun.*, 1982, 773; J. A. K. Howard, I. D. Salter and F. G. A. Stone, *Polyhedron*, 1984, **3**, 567; M. I. Bruce and B. K. Nicholson, *J. Organomet. Chem.*, 1983, **252**, 243; M. I. Bruce and B. K. Nicholson, *J. Chem. Soc., Chem. Commun.*, 1982, 1141.
25 A. J. Amoroso, B. F. G. Johnson, J. Lewis, A. D. Massey, P. R. Raithby and W.-T. Wong, *J. Organomet. Chem.*, 1992, **440**, 219.
26 O. Orama, *J. Organomet. Chem.*, 1986, **314**, 273; E. Sappa, *J. Organomet. Chem.*, 1988, **352**, 327; M. I. Bruce, M. L. Williams, J. M. Patrick and A. H. White, *J. Chem. Soc., Dalton Trans.*, 1985, 1229; M. I. Bruce, M. J. Liddell and E. R. T. Tiekink, *J. Organomet. Chem.*, 1990, **391**, 81.

Received 22nd February 1995; Paper 5/01066G